J|A|C|S
ARTICLES
Published on Web 02/17/2004

Efficient Yellow Electroluminescence from a Single Layer of a Cyclometalated Iridium Complex

Jason D. Slinker,[†] Alon A. Gorodetsky,[†] Michael S. Lowry,[‡] Jingjing Wang,[‡] Sara Parker,[†] Richard Rohl,[†] Stefan Bernhard,*[,‡] and George G. Malliaras*[,†]

Contribution from the Department of Materials Science and Engineering, Cornell University, Ithaca, New York 14853, and Department of Chemistry, Princeton University, Princeton, New Jersey 08544

Received February 5, 2003; E-mail: sbernhar@princeton.edu; george@ccmr.cornell.edu

Abstract: We report on the spectroscopic, electrochemical, and electroluminescent properties of $[Ir(ppy)_2(dtb\text{-}bpy)]^+(PF_6)^-$ (ppy: 2-phenylpyridine, dtb-bpy: 4,4′-di-*tert*-butyl-2,2′-dipyridyl). Single-layer devices were fabricated and found to emit yellow light with a brightness that exceeds 300 cd/m^2 and a luminous power efficiency that exceeds 10 Lm/W at just 3 V. The PF_6^- space charge was found to dominate the device characteristics.

Introduction

Chelated ruthenium(II) complexes, such as $[Ru(bpy)_3]^{2+}(PF_6^-)_2$ (where bpy is 2,2′-bipyridine), have attracted a great deal of interest in the past few years as multifunctional chromophores for single-layer, solid-state electroluminescent devices.[1−6] In these devices, electrons and holes injected from two electrodes into a single layer of the ruthenium complex recombine, giving rise to light emission. External quantum efficiencies up to 5.5% have been achieved,[4] which rival those from multilayer devices whose fabrication is more complex, requiring several layers for charge injection, transport, and light emission. What makes this class of materials different from the other organic semiconductors typically used in solid-state electroluminescent devices is the presence of mobile ions: $[Ru(bpy)_3]^{2+}$ carries a 2+ net positive charge, which is balanced by two negative counterions, such as PF_6^-. These counterions drift under the influence of an applied bias, leading to accumulation of negative ionic charge near one electrode and depletion near the other electrode. This ionic space charge creates high electric fields at the electrodes, which enhances electronic charge injection into the transition-metal complexes. As a result, devices based on a single layer of such transition-metal complexes operate at a low voltage and have been shown to be rather insensitive to the choice of electrode material, allowing the use of air-stable anodes and cathodes.[1]

As with any new class of electroluminescent materials, these multifunctional chromophores must be shown to yield devices of high efficiency, sufficient stability, and various colors of emission for such materials to be considered promising candidates in display applications. Tuning of the color to achieve red, green, and blue emission is a particularly important feature of any new chromophore class, as mixing these colors produces white—a prerequisite for display and lighting applications. All single-layer devices from ruthenium chromophores reported thus far emit in the orange-red part of the spectrum.[1−6] Exploring different metal centers might provide a pathway to color tuning in this class of materials.

Changing the metal center to a more stable third-row transition metal is also a clear option for improving chromophore stability. This change not only dramatically improves the metal−ligand bond stability, but also increases the ligand field splitting energy (LFSE), rendering the dissociative e_g orbitals less accessible and leading to an enhancement of the photostability compared to ruthenium complexes. In this spirit, multifunctional complexes of osmium,[7] as well as rhenium,[8] have already been tried in single-layer electroluminescent devices. Complexes of iridium have been used extensively to produce highly efficient organic electroluminescent devices.[9−11] However, these were mainly in the neutral form (as opposed to the charged one which will be discussed here) and have been used primarily as emitters in multilayer devices, rather than as multifunctional chromophores. In this article, we report on a charged iridium complex, $[Ir(ppy)_2(dtb\text{-}bpy)]^+(PF_6^-)$ and its use as a multifunctional chromophore for single-layer electroluminescent devices. Two cyclometalating ligands (ppy: 2-phenylpyridine) were chosen to coordinate the iridium metal center to further increase the

[†] Cornell University.
[‡] Princeton University.

(1) Slinker, J.; Bernards, D.; Houston, P. L.; Abruña, H. D.; Bernhard, S.; Malliaras, G. G. *Chem. Commun.* **2003**, *19*, 2392.
(2) Handy, E. S.; Pal, A. J.; Rubner, M. F. *J. Am. Chem. Soc.* **1999**, *121*, 3525.
(3) Gao, F. G.; Bard, A. J. *J. Am. Chem. Soc.* **2000**, *122*, 7426.
(4) Rudmann, H.; Shimada, S.; Rubner, M. F. *J. Am. Chem. Soc.* **2002**, *124*, 4918.
(5) Buda, M.; Kalyuzhny, G.; Bard, A. J. *J. Am. Chem. Soc.* **2002**, *124*, 6090.
(6) Bernhard, S.; Barron, J. A.; Houston, P. L.; Abruña, H. D.; Ruglovsky, J. L.; Gao, X.; Malliaras, G. G. *J. Am. Chem. Soc.* **2002**, *124*, 13624.
(7) Bernhard, S.; Gao, X.; Abruña, H. D.; Malliaras, G. G. *Adv. Mater.* **2002**, *14*, 433.
(8) Gong, X.; Ng, P. K.; Chan, W. K. *Adv. Mater.* **1998**, *10*, 1337.
(9) Baldo, M. A.; O'Brien, D. F.; You, Y.; Shoustikov, A.; Sibley, S.; Thompson, M. E.; Forrest, S. R. *Nature* **1998**, *395*, 151.
(10) Adachi, C.; Kwong, R. C.; Djurovich, P.; Adamovich, V.; Baldo, M. A.; Thompson, M. E.; Forrest, S. R. *Appl. Phys. Lett.* **2001**, *79*, 2082.
(11) Adachi C.; Baldo, M. A.; Thompson, M. E.; Forrest, S. R. *J. Appl. Phys.* **2001**, *90*, 5048.

LFSE. The third ligand in the studied chromophore, 4,4′-di-*tert*-butyl-2,2′-dipyridyl (dtb-bpy), ensures redox reversibility, decreases self-quenching, and enhances device characteristics. We discuss the spectroscopic, electrochemical, and electroluminescent properties of this material.

Experimental Section

Solvents and reagents for synthesis were purchased from Aldrich and used without further purification. Acetonitrile (Fluka, puriss, anhydrous, over molecular sieves) and Tetra-*n*-butylammonium hexafluorophosphate (TBAH) (Fluka, electrochemistry grade) were used for the spectroscopic and electrochemical experiments. Redox potentials (vs Ag/AgCl) were determined using an Analytical Instruments Systems Inc. DLK-60 potentiostat. The redox potentials were determined through cyclic voltammetry employing a 0.2 mM solution of the iridium complex in a 0.1 M solution of tetra-*n*-butylammonium hexafluorophosphate with a Pt disk electrode (surface: 0.79 $(mm)^2$) at a scan rate of 100 mV/s. A Varian Inova-500 spectrometer was used to collect ^1H and ^{13}C NMR data. The photophysical measurements were carried out on a Photon Technology International Quantamaster and Timemaster system equipped for steady-state and time-resolved emission spectroscopy. The samples (0.01 mM in acetonitrile) were deaerated with nitrogen and excited at 400 nm (steady-state) or 355 nm (time-resolved). The emission quantum yields (Φ_{em}) were measured relative to $[Ru(bpy)_3]^{2+}(PF_6^-)_2$.

The synthesis of $[Ir(ppy)_2(dtb\text{-}bpy)]^+(PF_6^-)$ was adapted from literature procedures for the analogous unsubstituted complex.[12] A magnetically stirred suspension of 4,4′-di-*tert*-butyl-2,2′-dipyridyl (118 mg, 0.44 mmol) and tetrakis(2-phenylpyridine-C^2,N′)(μ-dichloro)-diiridium (214 mg, 0.2 mmol) in 10 mL of 1,2-ethanediol under nitrogen was heated to 150 °C. The mixture was kept at this temperature for 15 h. All the solids dissolved to yield a clear, yellow solution. After cooling the mixture to room temperature, 150 mL of water was added. The excess of bipyridine ligand was removed through three extractions with diethyl ether (50 mL), and the aqueous layer was subsequently heated to 60−70 °C. NH_4PF_6 (1 g) in 10 mL of water was added, and the PF_6 salt of the chromophore immediately precipitated. After cooling the suspension to 5 °C, the yellow solid was separated through filtration, dried, and recrystallized through acetonitrile/ether diffusion.

Yield: 280 mg (77%). Analytical data. ^1H NMR (acetone-d_6, 500 MHz): δ 8.91 (dtb-bpy-H_3, 2H, d, $J = 1.83$ Hz), 8.27 (ppy-H_6, pyridine, 2H, dd, $J = 8.42$, 0.73 Hz), 8.01 (dtb-bpy-H_6, 2H, d, $J = 5.86$ Hz), 7.98 (ppy-H_5, pyridine, 2H, dt, $J = 8.42$, 1.46 Hz), 7.92 (ppy-H_3, phenyl, 2H, dd, $J = 8.06$, 1.09 Hz), 7.82 (ppy-H_6, phenyl, 2H, d, $J = 4.76$ Hz), 7.74 (dtb-bpy-H_5, 2H, dd, $J = 5.86$, 1.83 Hz), 7.16 (ppy-H_4, pyridine, 2H, dt, $J = 7.69$, 1.46 Hz), 7.06 (ppy-H_4, phenyl, 2H, dt, $J = 7.32$, 1.10 Hz), 6.94 (ppy-H_5, phenyl, 2H, dt, $J = 7.32$, 1.46 Hz), 6.37 (ppy-H_3, pyridine, 2H, dd, $J = 7.69$, 1.10 Hz), 1.44 (18H, s). ^{13}C NMR (acetone-d_6, 500 MHz): δ 168.2, 164.3, 156.2, 151.3, 150.5, 149.3, 144.3, 138.8, 131.8, 130.6, 125.8, 125.2, 123.7, 122.6, 122.2, 120.1, 35.8, 29.8. MS (*m*/*e*; ESI): 770 (100%, M − PF_6 + H^+). Elemental analysis: Calcd for $C_{40}H_{40}F_6IrN_4P\cdot H_2O$: C, 51.55; H, 4.54; N, 6.01. Found: C, 51.59; H, 4.57; N, 6.02.

Details on the device fabrication and characterization have been reported elsewhere.[6] In short, films of the iridium complex were spin-coated from an acetonitrile solution onto glass substrates covered with prepatterned ITO electrodes (Thin Film Devices, Anaheim, CA). The thickness of the films was between 70 and 90 nm, as measured with profilometry. The ITO substrates were cleaned just before the deposition of the organic layer by a deionized water bath, followed by UV/ozone treatment. The films were dried for approximately 12 h at 80 °C under vacuum and were introduced in a dry nitrogen glovebox for further processing and characterization. Either a 200-Å thick Au film or a 200-Å thick Ca film protected with a 200-Å thick Al film was used as cathodes and was deposited through a shadow mask that defined six devices per substrate with a 3-mm^2 active area each. The deposition of Au was carried out in an intermittent way to minimize heating of the organic film. The electrical characteristics of the devices were measured with a Keithley 236 source-measure unit, and the radiance measurements were collected with a calibrated UDT S370 optometer coupled to an integrating sphere. The electroluminescence spectra were measured with a calibrated S2000 Ocean Optics fiber spectrometer.

Results and Discussion

A strong emission can be observed from $[Ir(ppy)_2(dtb\text{-}bpy)]^+(PF_6^-)$ in an acetonitrile solution and as a spin-coated film. The luminescence peak maximum in solution (581 nm) indicates that the *tert*-butyl groups do not interfere with the photophysical properties of the parent compound $[Ir(ppy)_2(bpy)]^+(PF_6^-)$ (580 nm).[13] For a system that contains a combination of orthometalating and neutral ligands, such as $[Ir(ppy)_2(bpy)]^+(PF_6^-)$, both metal-to-ligand charge transfer (^{3}MLCT) and $^3\pi-\pi^*$ LC transitions are feasible. It is difficult to discern between these two transition types because they have similar energy, and the emitted light conveys properties unique to both (i.e., the intensity and band shape of the emitted light correspond to a $^3\pi-\pi^*$ transition, but the lifetime and oscillator strength correspond to a ^{3}MLCT). Güdel et al. conclude, therefore, that emission in these mixed-ligand systems can actually be attributed to strong mixing between the MLCT and LC excited states.[14,15] Comparison of the luminescence spectra in solution and measured from a spin-coated film (peak maximum: 558 nm) indicate that the emission maximum strongly depends on the environment. This result is supported by the observation that the emission of the unsubstituted $[Ir(ppy)_2(bpy)]^+(PF_6^-)$ exhibits emission shifts of 80 nm from solid-state to solution.[13]

$[Ir(ppy)_2(dtb\text{-}bpy)]^+(PF_6^-)$ exhibits a room-temperature emission quantum yield Φ_{em} almost 4 times as high as the one observed for $[Ru(bpy)_3]^{2+}(PF_6^-)_2$. The stronger ligand field of the ppy ligand, the higher charge of the iridium, and the switch from a second-row to a third-row transition-metal center lead to a substantial increase in LFSE, rendering the radiationless deactivation pathway through dissociative metal-centered d−d states much less favorable. The shorter emission lifetime of the iridium complex compared to that of $[Ru(bpy)_3]^{2+}(PF_6^-)_2$ is contrary to this increase in quantum efficiency. However, the increased spin−orbit coupling in third-row transition-metal complexes accelerates radiative and nonradiative singlet−triplet transitions, thereby decreasing the duration of their excited-state lifetime. This fact is well-documented in comparative studies on ruthenium and osmium trisdiimine complexes.[16,17]

The emission lifetimes for acetonitrile solutions of both complexes in an air and in a nitrogen atmosphere are tabulated in Table 1. Analogous to the efficient emission quenching in $[Ru(bpy)_3]^{2+}(PF_6^-)_2$, which is attributed to an energy-transfer mechanism, a 10-fold increase in fluorescence lifetime is observed for $[Ir(ppy)_2(dtb\text{-}bpy)]^+(PF_6^-)$ upon deaerating.[18]

(12) Sprouse, S.; King, K. A.; Spellane, P. J.; Watts, R. J. *J. Am. Chem. Soc.* **1984**, *106*, 6647.
(13) King, K. A.; Watts, R. J. *J. Am. Chem. Soc.* **1987**, *109*, 1589−1590.
(14) Colombo, M. G.; Hauser, A.; Güdel, H. U. *Inorg. Chem.* **1993**, *32*, 3088−3092.
(15) Colombo, M. G.; Güdel, H. U. *Inorg. Chem.* **1993**, *32*, 3081−3087.
(16) Adamson, A. W.; Fleischauer, P. D. *Concepts in Inorganic Photochemistry*; Wiley & Sons: New York, 1975; p 206ff.
(17) Kober, E. M.; Casper, J. V.; Lumpkin, R. S.; Meyer, T. J. *J. Phys. Chem.* **1986**, *90*, 3722.
(18) Kaizu, Y.; Ohta, H.; Kobayashi, H.; Kobayashi, K.; Takuma, K.; Matsuo, T. *J. Photochem.* **1985**, *30*, 93.

Table 1. Comparison of the Solution (10 μM in Acetonitrile) Photophysical Properties of $[Ir(ppy)_2(dtb\text{-}bpy)]^+(PF_6^-)$ to Those of $[Ru(bpy)_3]^{2+}(PF_6^-)_2$

compound	emission maximum	emission quantum yield	luminescence lifetime in air	luminescence lifetime in N_2
$[Ir(ppy)_2(dtb\text{-}bpy)]^+(PF_6^-)$	581 nm	0.235	65 ns	557 ns
$[Ru(bpy)_3]^{2+}(PF_6^-)_2$	605 nm	0.062[19]	153 ns	810 ns (lit. 870 nm)[18]

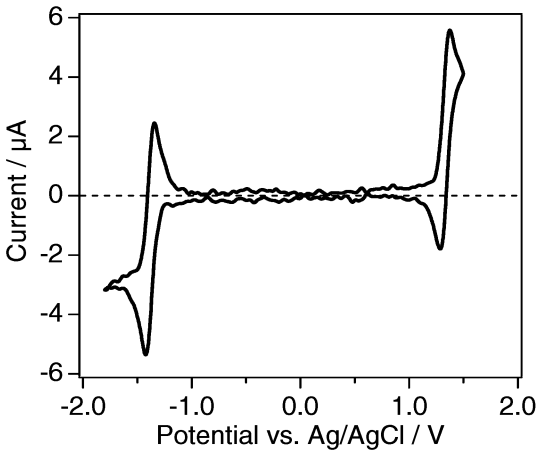

Figure 1. Cyclic voltammogram for a Pt electrode in contact with a 0.10 M TBAH/AN solution containing 0.2 mM $[Ir(ppy)_2(dtb\text{-}bpy)]^+$. The scan rate was 100 mV/s.

Table 2. Redox Potentials vs Ag/AgCl Obtained from the Cyclic Voltammograms for a Pt Electrode in Contact with a 0.10 M TBAH/AN Solution of 0.2 mM Metal Complex at 100 mV/s

compound	$M^{n+}/M^{(n+1)+}$ $E^{1/2}$ (V) [ΔE (mV)]	(ligand/ligand$^-$) $E^{1/2}$ (V) [ΔE (mV)]		
		1	2	3
$[Ir(ppy)_2(dtb\text{-}bpy)]^+(PF_6^-)$	1.33 [83]	−1.38 [75]		
$[Ru(bpy)_3]^{2+}(PF_6^-)_2$	1.34 [79]	−1.28 [61]	−1.45 [70]	−1.68 [69]

The redox behavior in acetonitrile is characterized through a one-electron oxidation of the iridium center at +1.33 V vs Ag/AgCl and a one-electron reduction of the 2,2′-bipyridine at −1.38 V vs Ag/AgCl. Both redox processes are highly reversible, with a wave-shape that is characteristic of a diffusional process. Figure 1 depicts the cyclic voltammogram of the complex in acetonitrile solution at a scan rate of 100 mV/s. The peak integration of a differential pulse polarogram (DPP) is used to establish the one-electron character of the redox reactions. Table 2 compares the redox behavior of $[Ir(ppy)_2(dtb\text{-}bpy)]^+(PF_6^-)$ with that of $[Ru(bpy)_3]^{2+}(PF_6^-)_2$. The increase in the optical gap achieved in the Ir complex arises primarily through a reduction in the electron affinity.

The electroluminescence spectra from an ITO/$[Ir(ppy)_2(dtb\text{-}bpy)]^+(PF_6^-)$/Au device under forward (ITO biased positively) and reverse bias are shown in Figure 2. The spectrum obtained under forward bias is centered at 560 nm and is nearly identical to the film photoluminescence (centered at 558 nm), indicating that the same optical transition is responsible for light emission. On the other hand, a red shift of 20 nm is observed in the emission of all devices under reverse bias. The origin of this spectral shift is further discussed below. The CIE coordinates are $x = 0.425$, $y = 0.549$ for forward bias and $x = 0.491$, $y = 0.496$ for reverse.

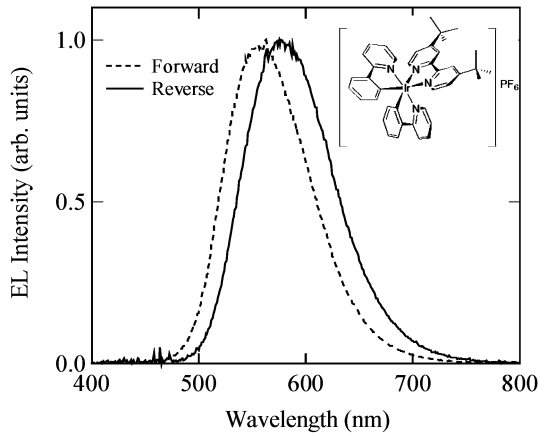

Figure 2. ITO/$[Ir(ppy)_2(dtb\text{-}bpy)]^+(PF_6^-)$/Au emission spectrum. Inset: Chemical structure of $[Ir(ppy)_2(dtb\text{-}bpy)]^+(PF_6^-)$.

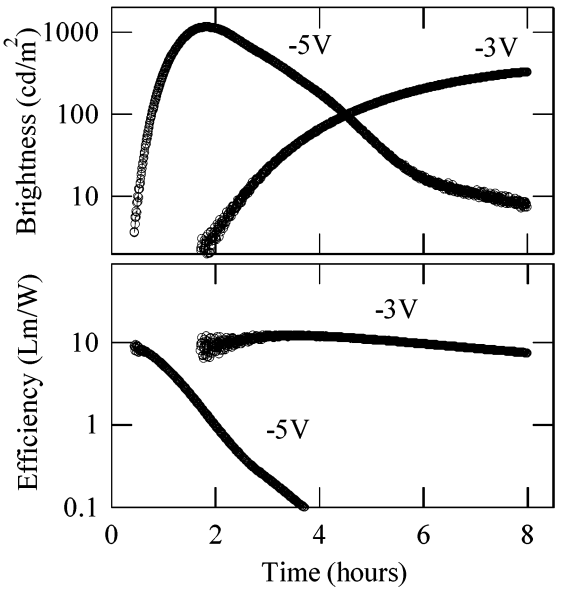

Figure 3. Brightness and luminous efficiency of ITO/$[Ir(ppy)_2(dtb\text{-}bpy)]^+(PF_6^-)$/Au devices under reverse bias.

The electrical characteristics of the ITO/$[Ir(ppy)_2(dtb\text{-}bpy)]^+(PF_6^-)$/Au devices are found to be similar to those seen in devices from analogous ruthenium and osmium complexes.[1−7] Namely, a time-delayed rather than an instant response is observed upon application of a bias. This is shown in Figure 3, where the brightness of a device biased at −5 V (reverse bias) takes almost 2 h to reach its peak value. At −3 V, the emission keeps increasing even after 8 h. This delayed response reflects the mechanism of device operation, which involves drift and accumulation of the PF_6^- ions near the positively charged electrode. The ionic space charge leads to the buildup of a high electric field at both contacts. This, in turn, enhances electronic carrier injection and results in the observed increase in the device brightness.[20]

A remarkable feature of these devices is their high luminous power efficiency, which exceeds 10 Lm/W at −3 V. This is among the highest efficiencies observed in a single-layer OLED. It is close to the state of the art of 60 Lm/W, measured in devices

(19) Calvert, J. M.; Caspar, J. V.; Binstead, R. A.; Westmoreland, T. D.; Meyer, T. J. *J. Am. Chem. Soc.* **1982**, *104*, 6620.
(20) deMello, J. C.; Tessler, N.; Graham, S. C.; Friend, R. H. *Phys. Rev. B* **1998**, *57*, 12951.

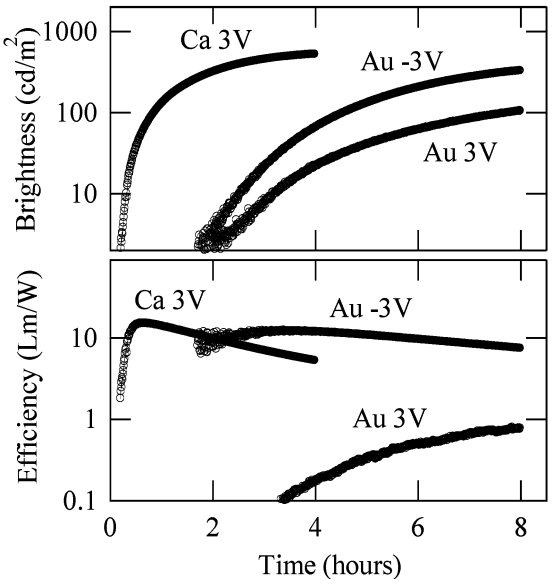

Figure 4. Brightness and luminous efficiency of ITO/$[Ir(ppy)_2(dtb\text{-}bpy)]^+(PF_6^-)$ devices with Au and Ca cathodes.

that employ five layers between the electrodes.[21] The brightness of these devices is equally impressive, reaching 330 cd/m^2 at just −3 V. The external quantum efficiency at the same voltage reaches 5%. It should be noted that ITO/$[Ru(bpy)_3]^{2+}(PF_6^-)_2$/Au devices of comparable thickness, prepared and characterized under identical conditions in our lab, showed a luminous efficiency of 0.3 Lm/W, a brightness of 440 cd/m^2, and an external quantum efficiency of 0.5% at 3 V.[6]

The efficiency of an ITO/$[Ir(ppy)_2(dtb\text{-}bpy)]^+(PF_6^-)$/Au device is shown in Figure 3 to decay at a rate that depends on the bias. This has been observed in devices from ruthenium as well as osmium complexes: The higher the voltage above the redox potential, the faster the degradation. The reasons for the degradation in the iridium complex-based devices are not completely understood at present. Systematic work from the Bard group[22] led to the conclusion that degradation in $[Ru(bpy)_3]^{2+}$ arises from a reaction with water and the subsequent production of $[Ru(bpy)_2(H_2O)_2]^{2+}$, which decreases the yield of photoluminescence. A similar mechanism might be at work for $[Ir(ppy)_2(dtb\text{-}bpy)]^+(PF_6^-)$. It should be noted though that schemes to slow degradation in these devices are being developed.[4]

The characteristics of the ITO/$[Ir(ppy)_2(dtb\text{-}bpy)]^+(PF_6^-)$/Au devices are found to be highly asymmetric with bias (see Figure 4). Namely, the luminous efficiency at 3 V is considerably lower than that at −3 V. This is in contrast to past work on ruthenium devices, where ITO and Au were found to give ohmic contacts for both hole and electron injection, leading to absence of rectification.[6] The latter was attributed to the high electric field near the electrodes, caused by the redistribution of ionic charge.[20] Due to the lower electron affinity of the iridium complex, the field caused by the ionic space charge seems not to be adequate to make Au an ohmic contact for electron injection. As a result, ITO serves as a more efficient electron injector that Au. This is in agreement with the fact that the work function of ITO is lower than that of Au and suggests that higher efficiency devices might be achieved by using a cathode with a lower work function.

To test this hypothesis, devices were fabricated using a low work function cathode. Figure 4 compares the performance of devices with Au and Ca cathodes. The data are consistent with the fact that Ca is a more efficient electron injector than Au and ITO: The device with the Ca cathode turns on considerably faster and reaches a higher brightness and luminous efficiency than the devices where Au or ITO are used as electron injectors (data marked as Au 3 V and Au −3 V, respectively). The fact that the turn on time of the device with the Ca cathode is considerably shorter is consistent with the presence of a smaller barrier for electron injection: Fewer PF_6^- ions need to redistribute to establish efficient electron injection from Ca than from Au or ITO. It should be noted that the devices with Ca cathodes did not emit any light under reverse bias. A similar electrochemical degradation of Al electrodes under reverse bias was observed in $[Ru(bpy)_3]^{2+}(PF_6^-)_2$ devices.[23]

Unfortunately, the improvement achieved in the device performance by using a Ca cathode comes at the expense of electrode stability. The use of Ca removes one of the chief advantages of devices based on transition-metal complexes, namely their ability to yield efficient devices even with air stable electrodes. The present work shows that, contrary to the case of $[Ru(bpy)_3]^{2+}$, the ionic space charge in complexes with a larger HOMO/LUMO gap might not be enough to make every contact ohmic. This impacts not only the maximum device efficiency, but also the turn on time. However, it should be noted that there are several ways to improve the turn on time of devices based on transition-metal complexes. These include modifying the ligand,[2] using smaller, more mobile counterions,[4,5] as well as prebiasing the device at a higher voltage or driving it with a square wave.[4] Some of these strategies have also led to an enhancement of the efficiency in ruthenium-based devices. Therefore, it might be possible to achieve an even higher efficiency in $[Ir(ppy)_2(dtb\text{-}bpy)]^+(PF_6^-)$ devices using air stable contacts.

Finally, a comment is in order regarding the spectral shift of the emission. The emission spectrum of the device with the Ca cathode (under forward bias) shows a maximum at 580 nm, similar to that of the device with the Au cathode under reverse bias. This is red-shifted by 20 nm compared to the films photoluminescence and the electroluminescence spectrum from the device with a Au cathode under forward bias. This is a very interesting effect for which we currently have no explanation. The most obvious correlation of this spectral shift is with the luminous efficiency. When the efficiency is high (implying balanced electron and hole currents, as well as large concentration of excitons), the spectrum is shifted toward the red. Further studies of exciton-charge and exciton−exciton interactions in this material are needed to understand this interesting effect.

Conclusions

In conclusion, the spectroscopic, electrochemical, and electroluminescent properties of a multifunctional iridium complex have been discussed. Devices fabricated from $[Ir(ppy)_2(dtb\text{-}bpy)]^+(PF_6)^-$ emitted yellow light with a brightness exceeding

(21) Pfeiffer, M.; Forrest, S. R.; Leo, K.; Thompson, M. E. *Adv. Mater.* **2002**, *14*, 1633.
(22) Kalyuzhny, G.; Buda, M.; NcNeill, J.; Barbara, P.; Bard, A. J. *J. Am. Chem. Soc.* **2003**, *125*, 6272.
(23) Rudmann, H.; Shimida, S.; Rubner, M. F.; Oblas, D. W.; Whitten, J. E. *J. Appl. Phys.* **2002**, *92*, 1576.

300 cd/m^2 and a luminous power efficiency exceeding 10 Lm/W at just 3 V. Their performance was dominated by the redistribution of PF_6^- ions. This material is a promising candidate for applications in solid-state electroluminescent devices.

Acknowledgment. This work was supported by the National Science Foundation (Career Award DMR-0094047) and by the Cornell Center for Materials Research (CCMR), a Materials Research Science and Engineering Center of the National Science Foundation (DMR-9632275). S.B. gratefully acknowledges support from a Camille and Henry Dreyfus Foundation New Faculty Award.

JA0345221